Combined In Silico Modeling and Metabolomics Analysis to Characterize Fed-Batch CHO Cell Culture

Suresh Selvarasu,[1] Ying Swan Ho,[1] William P. K. Chong,[1] Niki S. C. Wong,[1] Faraaz N. K. Yusufi,[1] Yih Yean Lee,[1] Miranda G. S. Yap,[1,2] Dong-Yup Lee[1,2]

[1]Bioprocessing Technology Institute, Agency for Science, Technology and Research (A*STAR), 20 Biopolis Way, #06-01, Centros, Singapore 138668, Singapore; telephone: +65-6516-6907; fax: +65-6779-1936; e-mail: cheld@nus.edu.sg

[2]Department of Chemical and Biomolecular Engineering, National University of Singapore, 4 Engineering Drive 4, Singapore 117576, Singapore

ABSTRACT: The increasing demand for recombinant therapeutic proteins highlights the need to constantly improve the efficiency and yield of these biopharmaceutical products from mammalian cells, which is fully achievable only through proper understanding of cellular functioning. Towards this end, the current study exploited a combined metabolomics and in silico modeling approach to gain a deeper insight into the cellular mechanisms of Chinese hamster ovary (CHO) fed-batch cultures. Initially, extracellular and intracellular metabolite profiling analysis shortlisted key metabolites associated with cell growth limitation within the energy, glutathione, and glycerophospholipid pathways that have distinct changes at the exponential-stationary transition phase of the cultures. In addition, biomass compositional analysis newly revealed different amino acid content in the CHO cells from other mammalian cells, indicating the significance of accurate protein composition data in metabolite balancing across required nutrient assimilation, metabolic utilization, and cell growth. Subsequent in silico modeling of CHO cells characterized internal metabolic behaviors attaining physiological changes during growth and non-growth phases, thereby allowing us to explore relevant pathways to growth limitation and identify major growth-limiting factors including the oxidative stress and depletion of lipid metabolites. Such key information on growth-related mechanisms derived from the current approach can potentially guide the development of new strategies to enhance CHO culture performance.

Biotechnol. Bioeng. 2012;109: 1415–1429.

© 2012 Wiley Periodicals, Inc.

Introduction

The majority of recombinant protein drugs currently available are predominantly produced by mammalian cells under various cell culture modes (Butler, 2005; Reff, 1993). In order to meet the increasing demand of such biopharmaceutical products, significant efforts have been made for improving the recombinant protein production yield from mammalian cell cultures (Barnes and Dickson, 2006; Ma et al., 2009). Among available mammalian cell lines, Chinese hamster ovary (CHO) cells play a major role in the industrial production of recombinant therapeutics (Jayapal et al., 2007). To date, various approaches have been explored to enhance CHO culture performance by investigating the effect of genetic/environmental perturbation on the cell growth and productivity via changes in gene expression (Schaub et al., 2009), studying the correlation of glucose and lactate metabolism with cell density under different culture conditions (Tsao et al., 2005) and examining the impact of replacing glutamine with alternate carbon sources such as glutamate or pyruvate on the cell growth (Altamirano et al., 2001; Genzel et al., 2005). While these approaches help to characterize the functional behavior of CHO cells qualitatively, quantitative improvements may not be easily achieved due to the limited understanding of intracellular metabolic activities (Dinnis and James, 2005). To address this limitation, a number of

"-omics" profiling technologies such as transcriptomics (Schaub et al., 2009), proteomics (Yizhak et al., 2010), and most recently, metabolomics (Chong et al., 2009; Ma et al., 2009) have been utilized to gain a more in-depth insight into the complex mechanisms involved in the regulation of major cellular processes. Of the different "-omics" technologies, metabolomics analysis enabled us to directly identify key metabolites and pathways closely associated with growth limitation and apoptosis (Chong et al., 2011).

Concurrently, advances in genomic technologies have also led to the development of computational models of cellular organisms that allow for the systematic elucidation of their genotype–phenotype characteristics (Lee et al., 2005; Price et al., 2003). The primary requirement of these modeling approaches includes the incorporation of genome annotation, biochemical and cell physiological data (Ma and Zeng, 2003). Such models have been developed for a wide range of microbes (Covert et al., 2003; Lee et al., 2005; Price et al., 2004) and only a handful of mammalian systems such as *Homo sapiens*, *Mus musculus*, and *Cannis fabris* (Duarte et al., 2007; Price et al., 2004; Selvarasu et al., 2010a; Wahl et al., 2008). Indeed, these models have been successfully exploited in understanding the cell physiological activities of various microorganisms in conjunction with "-omics" data for biotechnological and biomedical applications within the context of systems biology (Lee et al., 2005; O'Callaghan and James, 2008). Similarly, for mammalian cell culture, it is now possible to combine in silico metabolic modeling with global "-omics" data for better understanding of cell culture processes at the extracellular and intracellular levels (Lee et al., 2006; Mo et al., 2009).

In this study, as illustrated in Figure 1, we present an integrated framework where CHO fed-batch culture data are analyzed and combined with metabolomics profiles, followed by in silico modeling and analysis of mammalian cells to investigate their metabolic states and cellular physiology during the culture (Selvarasu et al., 2010a).

Materials and Methods

Cell Lines and Media

CHO cell lines expressing recombinant monoclonal antibody (IgG) against Rhesus D antigen were in-house generated (Chusainow et al., 2009). CHO mAb M250-9 (M250-9) was a sub-clone derived from additional rounds of methothrexate (MTX) amplification at 250 nM. For the measurement of CHO cell composition, M250-9 cells were cultured in a mixture consisting of a 1:1 (v/v) ratio of HyQ PF-CHO (Hyclone, Logan, UT) and CD CHO (Gibco-Invitrogen, Carlsbad, CA) supplemented with 6 mM L-glutamine (Sigma–Aldrich, St. Louis, MO) and 0.05% (v/v) Pluronic® F-68 (Invitrogen, Carlsbad, CA). Additional 250 nM MTX (Sigma–Aldrich) was added to the culture. The cell line was maintained in a humidified incubator controlled at 37°C under 8% CO_2 overlay. In addition, other CHO cell lines (CHO mAb M500-7, CHO K1, CHO DG44, and CHO DXB11) were also prepared for biomass compositional analysis. The method to determine cell composition of these cell lines is described in Supplementary 1.

Bioreactor Operations

The cultures were conducted in a 5 L double-walled, round-bottom glass vessel (B. Braun, Melsungen, Germany) with a heated water jacket. The reactor was inoculated with a seeding density of 3×10^5 cells/mL at a working volume of 4 L. The bubble-less aeration was effected through the use of a silicon membrane tubing basket (B. Braun) and the dissolved oxygen (DO) concentration maintained at 50% of air saturation using an Air/N_2 mix (early phase) or O_2/Air mix (late phase) set at 1 L/min. The agitation rate was set at 120 rpm using a three-blade segmented impeller. The culture pH was maintained at 6.9 using intermittent CO_2 addition to the gas mix or 8.6% (w/v) $NaHCO_3$ (Sigma–Aldrich) solution.

The M250-9 cells were adapted to in-house proprietary protein-free, chemically defined (PFCD) media before the bioreactor runs and the protein-free feed was formulated based on a fortified 10× DMEM/F12 (Sigma–Aldrich). Glutamine and glutamate concentrations in the culture were tracked online using an automated aseptic online sampling loop as previously described (Lee et al., 2003). Online sampling of glutamine/glutamate level was done every 1.5 h with YSI 7100 biochemical analyzer (Yellow Springs Instruments, Yellow Springs, OH) and an online algorithm calculated the amount of concentrated feed required to maintain cultures at a pre-set glutamine level of 0.6 mM. Online oxygen uptake rate (OUR) estimation was done using the stationary liquid phase balance, maintaining a constant oxygen mass transfer coefficient (k_{LA}) across the aeration membrane via control of DO in the reactor at a fixed point (Miller et al., 1988). The overall mass transfer coefficient for oxygen across the aeration membrane, k_{LA}, was determined previously in a separate experiment (data not shown).

Cell Density Determination and Metabolite Analysis

Cell density was determined by cell counting using an improved Neubauer hemocytometer (Weber, England) and the viability of cells was estimated using the trypan blue exclusion method. The concentrations of glucose, lactate, glutamine, glutamate and ammonium in the culture supernatant were determined using YSI 7100 biochemical analyzer (Yellow Springs Instruments). Analysis of amino acids from supernatant samples was carried out by reverse-phase HPLC using a Shimpack VP-ODS column (Shimadzu, Japan) and detected at 395 nm using a fluorescent detector (Shimadzu). Amino acid derivatization prior to the HPLC analysis was performed using the Waters AccQ Fluor Reagent Kit (Millipore, Billerica, MA).
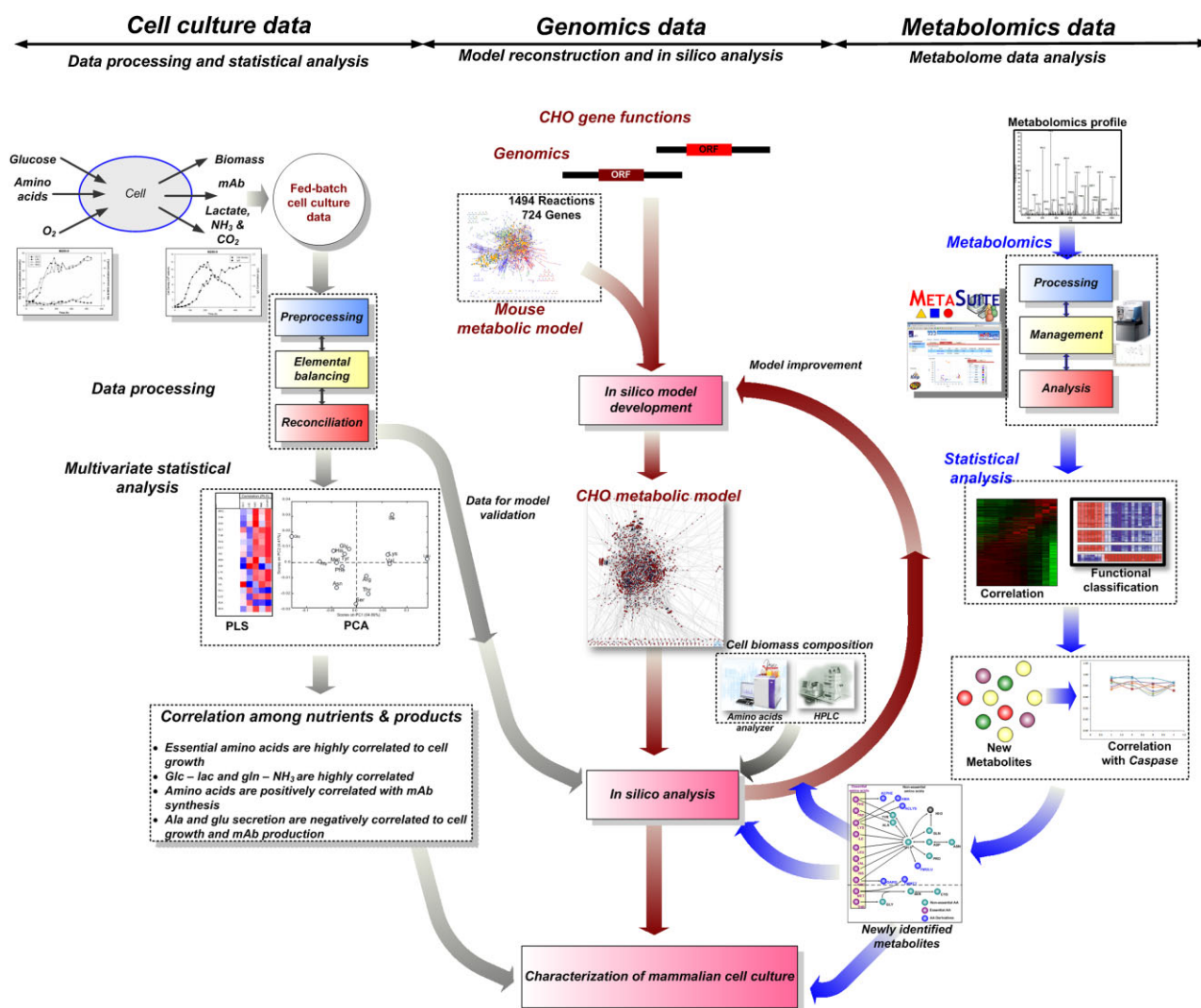
Figure 1. Schematic representation of combined framework involving statistical data analysis, in silico modeling and metabolomics analysis of CHO cell culture. Fed-batch data were initially preprocessed and statistical analysis was conducted to determine correlation among cell growth, nutrients, and toxic secretions. Concurrently, intracellular and extracellular metabolomics data analysis was performed to identify growth-limiting metabolites. Subsequently, CHO metabolic model was developed based on existing mouse model, in-house CHO cDNA annotation and metabolomics data. Then, the intracellular metabolic characteristics of CHO fed-batch culture was investigated by combining in silico modeling and metabolomics data analysis. [Color figure can be seen in the online version of this article, available at http://wileyonlinelibrary.com/bit]

Metabolomics Data Analysis

For extracellular metabolomics analysis, culture supernatant was obtained daily from replicate M250-9 fed-batch cultures and filtered through a 10 kDa molecular weight cut-off device (Vivaspin 500 PES membrane, Sartorius AG, Germany) by centrifugation at 4°C for 30 min. The filtered samples were diluted 1:1 with sample buffer comprising of 20% (v/v) methanol (Optima grade, Fisher Scientific, Singapore) in water prior to analysis.

For intracellular metabolomics analysis, 1×10^7 cells were obtained daily from the fed-batch cultures beginning at 24 h. The cells were quenched in five volumes of ice-cold 150 mM sodium chloride (Sigma–Aldrich) solution and centrifuged for 3 min at 1,250g and 4°C. The resulting solution was

aspirated and 400 μL of ice-cold methanol (Merck, Whitehouse Station, NJ) added to the cell pellet. The resuspended cells-methanol mixture was transferred to a 2 mL sample tube containing 200 μL of chloroform (J.T. Baker, Center Valley, PA). Subsequently, 900 μL of cold methanol, 3.8 mM tricine (Sigma–Aldrich) (9:10) mixture, and 400 μL of chloroform were added to the sample tube. The mixture was vortexed for 30 to 60 s after the addition of each solution. The sample was then centrifuged at 18,000g for 20 min at 4°C. 800 μL aqueous methanol–tricine layer was transferred to a clean tube. A further 700 μL of cold methanol and 3.8 mM tricine (9:10) mixture was added to the chloroform phase, which was then centrifuged at 18,000g for another 10 min at 4°C. 1 mL of the aqueous layer was extracted, combined with the first aqueous extract and

stored at −80°C. Prior to analysis, the aqueous extracts were dried and concentrated four times by adding the appropriate volume of sample buffer (20% methanol in water).

Both extracellular and intracellular samples were analyzed in replicates using an ultra performance liquid chromatography (UPLC) system (Acquity; Waters Corp., Milford, MA) coupled to a mass spectrometer (MS; LTQ-Orbitrap; Thermo Scientific, Bremen, Germany). A reversed phase (C18) UPLC column with polar end-capping (Acquity UPLC HSS T3 column, 2.1×100 mm, 1.7 μm; Waters Corp.) was used with two solvents: "A" being water with 0.1% formic acid (Merck), and "B" being methanol (Optima grade, Fisher Scientific, Pittsburgh, PA) with 0.1% formic acid. The UPLC program was as follows: the column was first equilibrated for 0.5 min at 0.1% B. The gradient was then increased from 0.1% B to 50% B over 8 min before being held at 98% B for 3 min. The column was washed for a further 3 min with 98% acetonitrile (Optima grade, Fisher Scientific) with 0.1% formic acid and finally equilibrated with 0.1% B for 1.5 min. The solvent flow rate was set at 400 μL/min; a column temperature of 30°C was used. The eluent from the UPLC system was directed into the MS. Electrospray ionization (ESI) was conducted in both positive and negative modes in full scan with a mass range of 80 to 1,000 m/z at a resolution of 15,000. Sheath and auxiliary gas flow was set at 40.0 and 15.0 (arbitrary units) respectively, with a capillary temperature of 400°C. The ESI source and capillary voltages were 4.5 kV and 40 V, respectively, for positive mode ionization, and 3.2 kV and −15 V, respectively, for negative mode ionization. Mass calibration was performed using standard LTQ-Orbitrap calibration solution (Thermo Scientific) prior to injection of the samples. The raw LC-MS data obtained was then preprocessed and analyzed using an in-house software which incorporated the XCMS peak finding algorithm (Smith et al., 2006). Detected mass peaks were assigned putative metabolite identities by matching the respective masses (< 10 ppm error) with the KEGG and Human Metabolome Database (HMDB). The pre-processed data was further analyzed using hierarchical clustering for the classification of common trends, which led to the identification of metabolites that were associated with cell growth. Where possible, the metabolite identities were confirmed by MS[2] spectral comparison with commercially available metabolite standards (all standards purchased from Sigma–Aldrich unless otherwise stated).

## Metabolic Network Development and In Silico Analysis

Recently available genome-scale metabolic model for mammalian cells accounts for 1,494 metabolic reactions, 724 ORFs and 715 enzymes (Selvarasu et al., 2010a). We expanded the network model by adding reactions obtained from CHO cDNA annotation, resulting in the addition of 35 new reactions from various metabolic subsystems. We also examined the model for missing links and improved the network connectivity by filling the gaps with necessary reactions that were identified based on metabolome analysis, while some reactions were excluded since their existence in CHO cell metabolism is not clear. As a result, we reconstructed a stoichiometrically balanced metabolic network model comprising 1,540 reactions and 1,302 metabolites (see Supplementary 2 for full list of reactions. The model is also available as Systems Biology Markup Language (SBML) file (level 2, version 1, http://sbml.org) in Supplementary 3. In addition to metabolic reactions, we included two balance equations representing biomass and IgG synthesis, both mainly composed of the biosynthetic precursors and relevant cofactors with appropriate coefficients, that are experimentally measured or obtained elsewhere for mammalian cells. Then, the steady state flux distributions across the network were quantitatively predicted by resorting to constraints-based flux analysis. The growth and non-growth conditions during the culture can be simulated by maximizing biomass and minimizing errors between experimental measurements and prediction, respectively, while satisfying thermodynamic and physicochemical constraints, using the linear programming technique (Edwards and Palsson, 1998). The detailed mathematical formulations pertinent to in silico analysis are available in Supplementary 1.

Results

Physiological Behavior of CHO Fed-Batch Cell Culture

Fed-batch bioreactor cultures of a CHO cell line producing recombinant monoclonal antibody (IgG) against Rhesus D antigen (M250-9) were conducted using an in-house proprietary protein free chemically defined medium. Concentrated feed media was supplied to the culture based on online monitoring of glutamine, with a set point of 0.6 mM to minimize the secretion of toxic metabolites like ammonia. The initial exponential (P1) and transition (P2) phases lasted until 190 h during which cell density reached a maximum of 1.2×10^7 cells/mL, followed by shift to short stationary phase (P3) up to 250 h and finally approaching death phase (Fig. 2A). The IgG concentration increased gradually during the exponential and stationary phase, reaching a maximum of 1.3 g/L after 260 h (Fig. 2A). Lactate and ammonia concentrations during the mid-exponential phase were 9.5 mM and 8.44 mM respectively, corresponding to secretion rates (P1) of 0.121 mmol/gDCW/h and 0.083 mmol/gDCW/h. During the exponential-stationary transition phase from 120 to 194 h, lactate and ammonia concentration increased significantly (secretion rates during P2 at 0.121 and 0.083 mmol/gDCW/h) and eventually reached a maximum of 39.5 mM g/L and 13.88 mM, respectively (Fig. 2B). Among various amino acids, alanine and glycine had the largest increases, while asparagine showed the most significant decrease as the fed-batch cultures progressed (Fig. 3A and C). Additionally, accumulation of
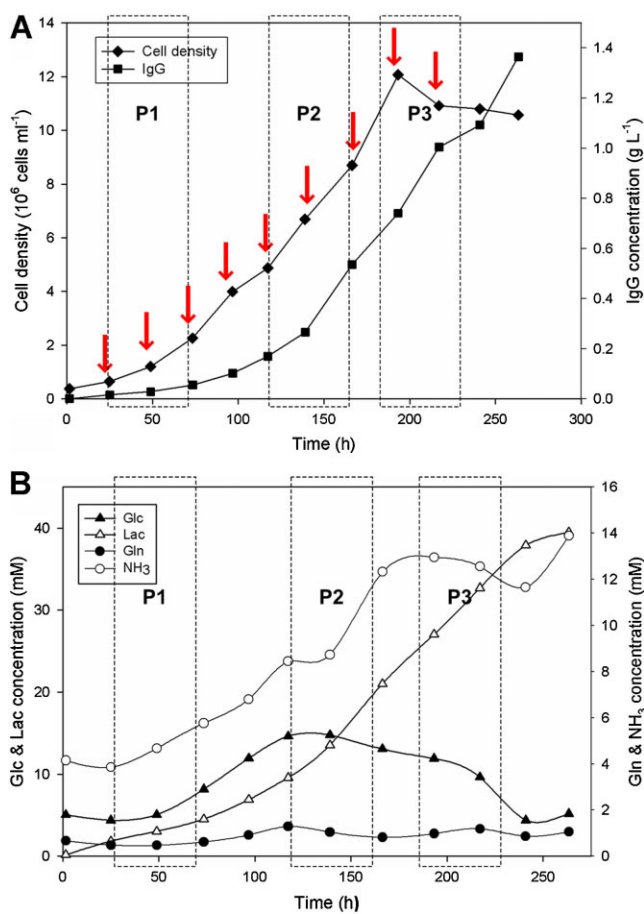
Figure 2. Time profiles of key CHO fed-batch bioreactor culture variables. Three distinct culture phases are shown, including initial exponential phase (P1), late exponential (transitional) phase (P2) and stationary phase (P3). **A**: Viable cell density and monoclonal antibodies (IgG) concentration profiles for the fed-batch cultures. Time points at which metabolomics samples were obtained for analysis are represented by arrows. **B**: Extracellular concentration profiles of major nutrients glucose (Glc), glutamine (Gln) and by-products lactate (Lac), and ammonia (NH₃). [Color figure can be seen in the online version of this article, available at http://wileyonlinelibrary.com/bit]
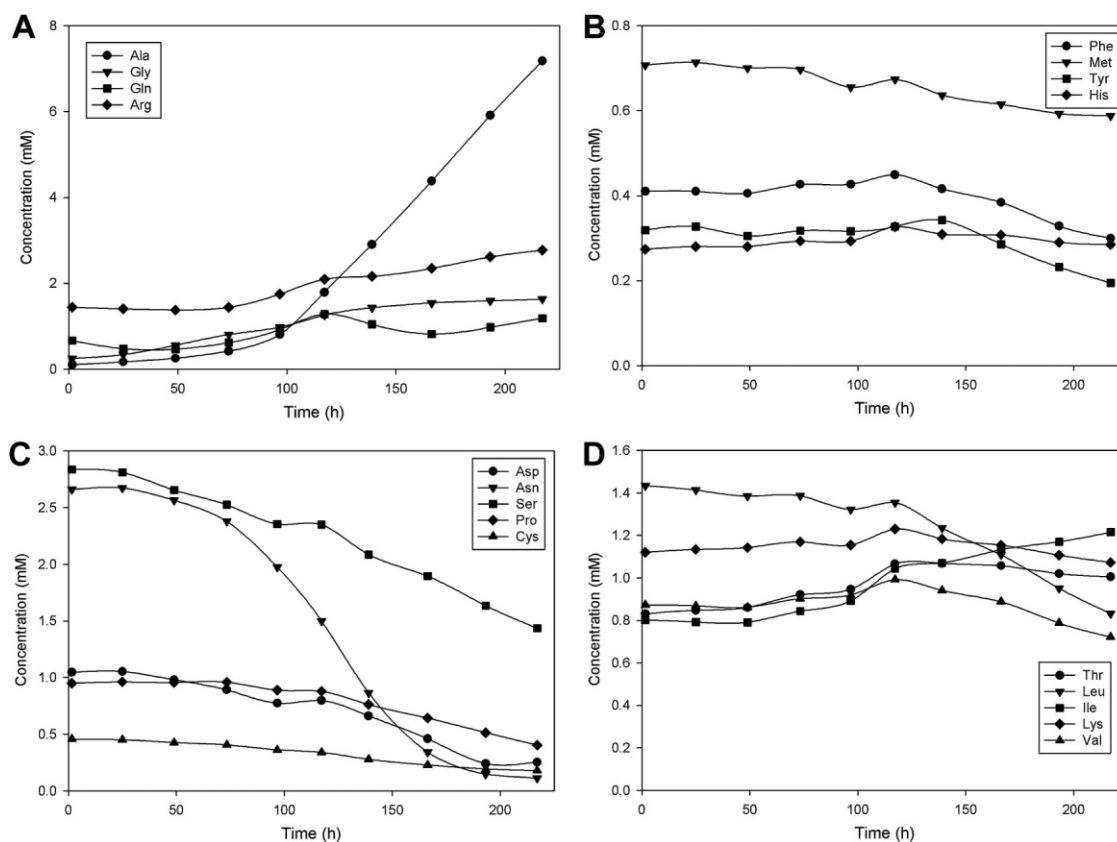
among the nutrient components, lactate and ammonia. The method for conducting these analysis techniques were adopted from Selvarasu et al. (2010b) (Supplementary 1). The results confirmed the expected correlation between glucose–lactate and glutamine–ammonia and also revealed an interesting correlation between ammonia and asparagine. Presumably, the conversion of asparagine via aspartate and glutamate could lead to the secretion of ammonia in the culture.

Extracellular Metabolite Profiling

Extracellular metabolite profiling was conducted on culture supernatant obtained daily from fed-batch cultures of the M250-9 cell line (Fig. 2A). The samples were processed using UPLC–MS and subsequently, trends of individual mass peaks were obtained using hierarchical clustering. The main objective of the analysis was to shortlist metabolites that are accumulated in the media over the progression of the cultures, as these represented compounds that could be potentially associated with growth-limitation or apoptosis. The information gained can be subsequently incorporated into the developed CHO metabolic model, which will be discussed later.

The specific cluster of mass peaks, which built up during the fed-batch cultures, is shown in Figure 4A. From the figure, the accumulation of these peaks appeared to coincide with the exponential-stationary transition phase (P2) of the cultures, suggesting that they were likely to be closely related to cell growth and apoptosis. A total of 100 mass peaks with putative identities were derived from both the positive and negative MS modes. From these masses, the identities of 19 metabolites were confirmed through MSMS spectral comparison with standard solutions (Table I). The majority of these metabolites can be categorized into three different compound classes—media components, amino acid derivatives, and nucleotides. Nine media components were found to accumulate extracellularly, suggesting that they were supplied in excess during the fed-batch cultures. The build-up of alanine, arginine, and glutamine reflects the amino acid trends observed in Figure 3A–D. Note that glycine was not detected as it had a molecular weight of <80 Da. Other media components identified included folic acid, nicotiamide, pantothenic acid, and riboflavin, indicating that feeding of these vitamins was in excess.

Of the six amino acid derivatives identified in the analysis, at least two were previously reported to be associated with apoptosis in other cell types. These include acetylphenylalanine (ACPHE), a harmful derivative present in the urine of phenylketonuria patients and dimethylarganine (DARG), known to induce apoptosis in endothelial cells (Jiang et al., 2006) by increasing intracellular reactive oxygen species production (Boger et al., 2000). In addition, the nucleotides AMP and GMP have also been known to arrest growth in

arginine was observed during the late exponential and non-growth phases, indicating excess supply of arginine from feed media during the stationary and cell death phases (Fig. 3A). From Figure 3C, asparagine was observed to be depleted significantly during the exponential phase despite continuous feeding of media. The higher consumption of asparagine had previously been shown to increase accumulation of alanine, glycine and ammonia in the media (Hansen and Emborg, 1994). It is therefore evident that the increasing secretion of alanine and glycine could be from asparagine conversion.

It should also be noted that the accumulation of lactate and ammonia inhibits the cell growth; hence, it is highly important to identify the relevant nutrients that contribute substantially to their secretion. To this end, we conducted multivariate statistical analysis using PCA and PLS on the cell culture profile that allows us to unravel the correlation

Figure 3. Extracellular concentration profiles of various amino acids over the course of the fed-batch culture. **A**: Gly, Ala, Gln, and Arg, **(B)** Phe, Met, Tyr, and His, **(C)** Asp, Ser, Asn, Pro, and Cys, and **(D)** Thr, Leu, Ile, Lys, and Val. Ala, alanine; Arg, arginine; Asn, asparagine; Asp, aspartate; Glc, glucose; Gln, glutamine; Glu, glutamate; Gly, glycine; His, histidine; Ile, isoleucine; Lac, lactate; Leu, leucine; Lys, lysine; Met, methionine; NH$_3$, ammonia; OUR, oxygen uptake rate; Phe, phenylalanine; Ser, serine; Thr, threonine; Tyr, tyrosine; and Val, valine.

CHO cells (Carvalhal et al., 2003) and apoptosis in IEC-6 intestinal epithelial cells (Chen et al., 2005).

Apart from the main compound classes, three other metabolites were identified. The accumulation of malic acid (MAL) was previously found to be a potential growth-limiting factor, attributed to the presence of an enzymatic bottleneck at malate dehydrogenase II, which catalyses the conversion of malic acid to oxaloacetate in the TCA cycle. Subsequent overexpression of the enzyme successfully improved cell growth and total product titre from CHO cells (Chong et al., 2010). Oxidized glutathione (GSSG) is a well-known marker for oxidative stress (Rossignol et al., 2007) and its build-up extracellularly suggests that reactive oxygen species are likely to be a key factor relating to growth-limitation and apoptosis. Additionally, GSSG was also known to induce apoptosis in U937 cells (Filomeni et al., 2003). Finally, glycerophosphocholine (G3PC) is a degradation product of phosphatidylcholine (PC) (Zablocki et al., 1991), a major constituent of the plasma membrane. The accumulation rate of G3PC increased sharply between 120 and 144 h, coinciding with the exponential-stationary transition phase (P2). This behavior indicated that there could be a corresponding increase in the degradation rate of

PC intracellularly, which would once again be associated with growth-limitation.

Intracellular Metabolite Profiling

An intracellular metabolite profiling study was also conducted on the M250-9 fed-batch cultures to identify important metabolic pathways that are closely associated with growth limitation. Cell samples were obtained daily during the cultures from 24 to 216 h (Fig. 2A) and processed using UPLC–MS. Similarly, the trends of individual mass peaks were obtained using hierarchical clustering. As the main focus of the study was on growth limitation, mass peaks showing a downward trend as the cultures progressed from the exponential (P1 and P2) to the stationary phase (P3) were shortlisted for further investigation (Fig. 4B). Among the resultant 42 mass peaks with putative identities, nine had their identities confirmed through MSMS spectral comparison with standard solutions and two were putatively identified based on accurate mass, as their standards were not commercially available (Table II). Interestingly, the metabolites were mostly components of three major
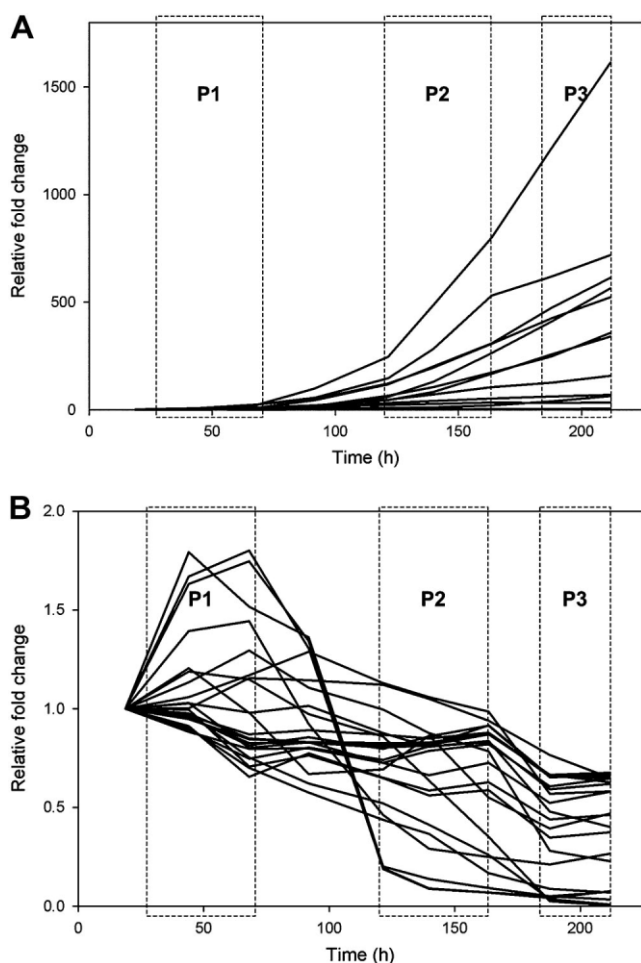
Figure 4. Selected trends associated with cell growth and apoptosis, derived from metabolomics analysis. **A**: Cluster of mass peaks with increasing trends over the course of the fed-batch culture obtained from extracellular metabolite profiling, (**B**) Cluster of mass peaks which decreased from the exponential (P1) to the stationary phase (P3) obtained from intracellular metabolite profiling.

pathways: energy, glutathione and glycerophospholipid metabolic pathways. This implied that the intracellular pools of metabolites in all three pathways were declining over the course of the culture. In particular, the intracellular levels of both reduced glutathione (GSH) and GSSG decreased progressively. The reduction in GSH seemed to support the hypothesis that the cells were experiencing oxidative stress. The decreasing trend of intracellular GSSG can be attributed to the attempt by the cells to maintain the intracellular GSH/GSSG ratio and hence, their redox potential. This appeared to be consistent with the observation that GSSG was being exported from the cells and accumulating in the extracellular media.

In glycerophospholipid metabolism, both choline phosphate (PCHO) and ethanolamine phosphate (PETHAM) decreased progressively, while CDP-choline (CDPCHO) and CDP-ethanolamine (CDPETN) were almost depleted intracellularly at around 144 h into the cultures (P2). The

two latter metabolites are the direct precursors for PC and phosphatidylethanolmine (PE), the major components of the plasma membrane. Their depletion appeared to be linked to the build-up of extracellular G3PC, at the exponential-stationary transition phase of the cultures. These observations strongly suggest that glycerophospholipid metabolism was closely associated with cell growth limitation. As such, an investigation of the internal metabolic flux changes in the glycerophospholipid metabolic pathway at different culture phases could help identify potential bottlenecks leading to growth limitation and subsequently contribute towards strategies to enhance culture viability.

In Silico Metabolic Modeling

The intracellular metabolic states of CHO cells grown in fed-batch culture can be examined using metabolic model of mammalian cells. Since recent efforts on sequencing and annotation of the CHO genome and gene function identification are still ongoing (Kantardjieff et al., 2009; Xu et al., 2011), alternatively, we used current generic metabolic models of mammalian cells as a template to analyze and characterize the metabolism of CHO cells. An initial set of enzymatic reactions for the CHO metabolic model was assembled based on genetic genome-scale mouse metabolic model (Selvarasu et al., 2010a). Subsequently, the model was further improved by including additional information from our in-house CHO cDNA annotation data. This led to the inclusion of 35 new gene-associated metabolic reactions. Metabolomics data analysis also contributed to the identification of additional metabolites and their respective enzymatic reactions as detailed in Table II, thereby improving the network connectivity of the CHO model. For instance, formylmethionine, a secretory metabolite, was identified based on the extracellular metabolite profiling study and subsequently included in the metabolic network as an additional reaction (EC: 3.5.1.31). Furthermore, transport reactions were included to reflect the accumulation of metabolites extracellularly. The list of additional genes and reactions is available in Supplementary 2. The resulting CHO metabolic model comprised of 1,540 enzymatic reactions and 1,302 metabolites categorized into two major compartments—the cytosol and mitochondria, besides the addition of reactions for transport of metabolites across the membranes.

Cellular biomass composition is an important prerequisite for in silico analysis, particularly during the exponential growth phase, where the primary objective of the cells is to maximize biomass growth. Until recently, many studies often assumed that cell biomass composition is conserved across closely related species. For instance, most of mammalian cell culture studies utilized the biomass composition derived from mouse hybridoma cells without any doubt (Altamirano et al., 2001). However, the biomass composition may vary across different species and is also

Table I. List of metabolites accumulating in the extracellular media over time.

Metabolite identity	MS polarity	Observed mass (m/z)	Theoretical mass (m/z)	Mass error (ppm)
Media components				
Folic acid (FOL)	+	442.1469	442.1469	−0.02
L-alanine (ALA)*	+	90.0546	90.0550	4.95
L-arginine (ARG)	+	175.1186	175.1190	2.01
L-glutamine (GLN)	−	145.0624	145.0619	−3.36
L-tryptophan (TRP)	+	205.0967	205.0972	2.36
Nicotinamide (NAM)	+	123.0550	123.0553	2.82
Pantothenic acid (PNTO)	+	220.1178	220.1179	0.47
Riboflavin (RIBFLAV)	+	377.1454	377.1455	0.30
Amino acid derivatives				
5-L-glutamyl-L-alanine (GALA)	−	217.0836	217.0830	−2.76
dimethyl-L-arginine (DARG)	+	203.1502	203.1503	0.72
N-acetyl-L-leucine (ACLEU)	−	172.0986	172.0979	−4.06
N-acetyl-L-phenylalanine (ACPHE)	+	208.0968	208.0968	0.02
N-acetylmethionine (ACMET)	−	190.0552	190.0543	−4.82
N-formyl-L-methionine (FMMET)	−	176.0392	176.0387	−2.87
Nucleotides				
AMP	−	348.0703	348.0704	0.37
GMP	−	362.0516	362.0507	−2.43
Other metabolites				
Glycerophosphocholine (G3PC)	+	258.1099	258.1106	2.67
Malic acid (MAL)	−	133.0148	133.0142	−4.48
Oxidized glutathione (GSSG)	−	611.1469	611.1447	−3.60

*The mass of L-alanine was too small for MS–MS fragmentation. Its identity was confirmed by accurate mass and retention time comparison with its standard.

likely to change under varying nutrient conditions. Previous studies have reported that incorporating inaccurate cell biomass composition into metabolic models could lead to erroneous conclusions when examining the metabolic activities (Carnicer et al., 2009; Raghunathan et al., 2003). Therefore, we conducted amino acids analysis on total cell proteins for five different CHO cell lines (M250-9, M500-7, CHO DG44, CHO DXBII, and CHO KI) to investigate their variations within CHO cells and difference with other mammalian cells (see Supplementary 1 for experimental method). The percentage of total cellular proteins in biomass was assumed to be same for all the cell lines. As

expected, comparison of amino acids composition among CHO cell lines could not reveal significant differences (Fig. 5A). However, when the amino acids composition of CHO cells was compared with that of mouse hybridoma cells (Bonarius et al., 1996; Selvarasu et al., 2009; Xie and Wang, 1994; Zupke and Stephanopoulos, 1995; Fig. 5B), surprisingly, we found significant changes in the compositions of lysine, glutamate, aspartate, and proline (Fig. 5C). In addition, the PCA results revealed two distinct clusters, (i) CHO cells and (ii) hybridoma mouse cells (Fig. 5D), implying that the amino acids content in total cell protein is likely to vary across different mammalian cell types. The

Table II. List of confirmed intracellular metabolites with a downward trend as the cultures progress.

Metabolite identity	MS polarity	Observed mass (m/z)	Theoretical mass (m/z)	Mass error (ppm)
Glycerophospholipid pathway metabolites				
CDP-choline (CDPCHO)	+	489.1134	489.1146	2.38
CDP-ethanolamine (CDPETN)*	−	445.0538	445.0538	−0.09
Choline phosphate (PCHO)	+	184.0728	184.0739	5.81
Ethanolamine phosphate (PETHAM)	−	140.0124	140.0118	−4.06
Energy pathway metabolites				
Citric acid (CIT)	−	191.0201	191.0197	−2.29
Malic acid (MAL)	−	133.0148	133.0142	−4.54
Oxalosuccinic acid (OSUC)*	−	189.0053	189.0041	−6.41
ADP	−	426.0231	426.0231	0.10
Glutathione pathway metabolites				
Oxidized glutathione (GSSG)	−	611.1462	611.1447	−2.53
Reduced glutathione (GSH)	+	308.0905	308.0911	2.08
Other metabolites				
Aspartic acid (ASP)	−	132.0308	132.0302	−4.90

*No standards are commercially available for these compounds. They were identified putatively based on accurate mass.
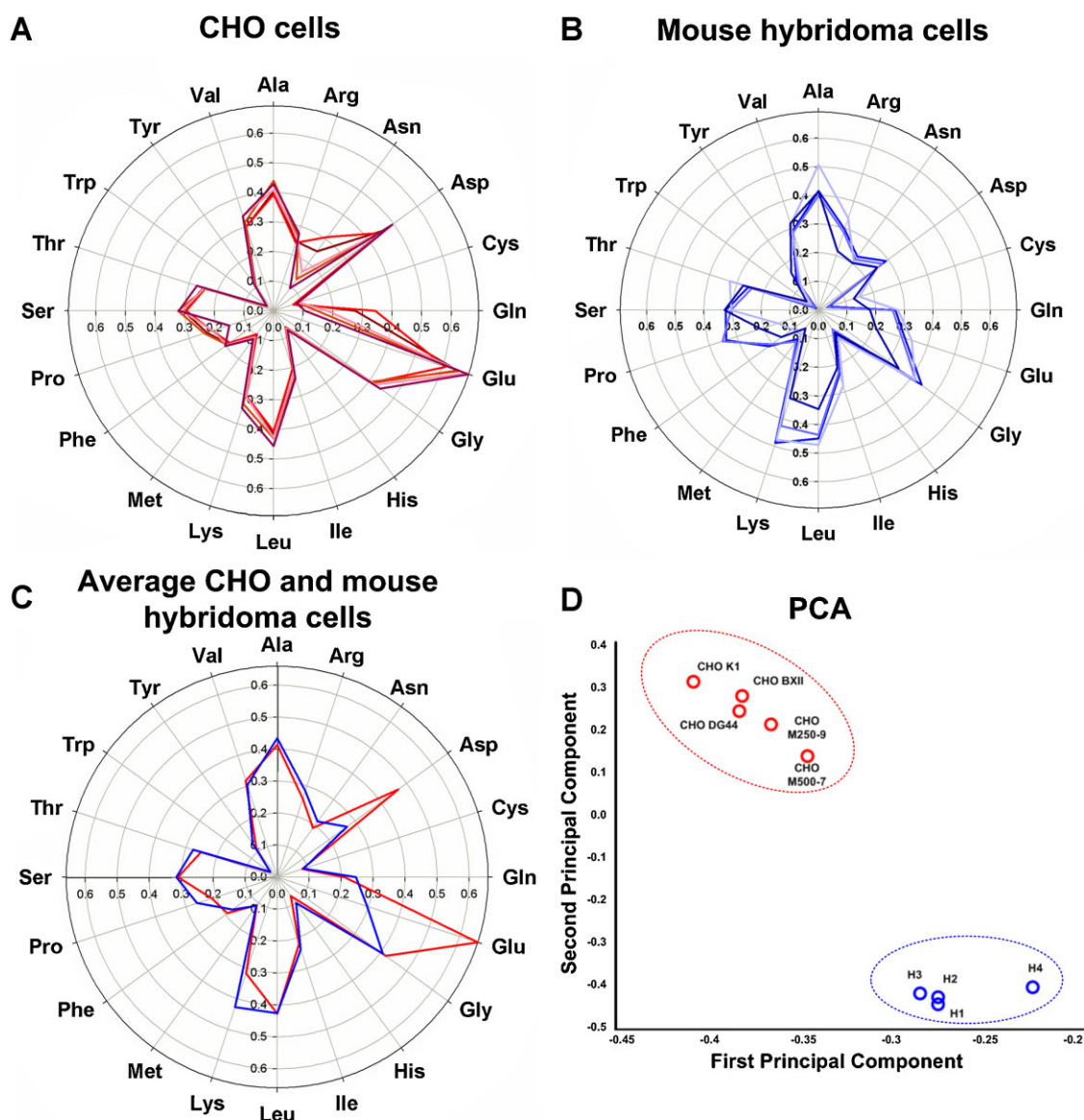
Figure 5. Amino acids composition in total cell proteins for various mammalian cells. **A**: CHO cell lines, (**B**) mouse hybridoma cell lines. **C**: average amino acids composition in CHO (red) and mouse hybridoma cells (blue). **D**: Principal component analysis of amino acid composition in the total cell proteins of CHO and mouse hybridoma cell lines. [Color figure can be seen in the online version of this article, available at http://wileyonlinelibrary.com/bit]

results also clearly highlight the need for a cautious approach in deriving the cell biomass equation for a specific cell type, especially while calculating the amino acids composition in total cell proteins for metabolite balancing.

In Silico Simulation of Metabolic Behavior during Growth and Non-Growth Phases

The intracellular metabolic characteristics of CHO cell lines producing monoclonal antibodies (IgG) were examined using the metabolic model under both exponential growth and non-growth phases. This could possibly explain

unique features of the varying metabolic states during the culture.

Initial and Late Exponential Phases

The major cellular objective in the exponential phase of a culture is to maximize cell growth. Thus, the metabolic model can be simulated to mimic the experimental conditions by maximizing cell growth rate subjected to constraints such as nutrient uptake rates and by-product production rates. For this, the uptake rates of nutrients, glucose, glutamine, amino acids and oxygen and secretion rates of cell biomass, IgG, ammonia, lactate and CO_2 were

calculated from the residual concentration data by following the general procedure (Selvarasu et al., 2010b). In silico simulations were carried out during initial (P1) and late (P2) exponential phases. When the experimental amino acids composition of total cell proteins in CHO M250-9 was considered in the biomass equation, simulated growth rates (P1: 0.0249/h; P2: 0.0106/h) matched very well with experimental growth rate (P1: 0.0247/h, P2: 0.0116/h) (Fig. 6). However, discrepancy between measured and predicted growth rates was observed when we used amino acids content from other mammalian cells (P1: 0.0171/h, P2: 0.008/h). Again, the results confirmed the need for having accurate CHO-specific biomass composition for reliable in silico analysis. We further explored the intracellular metabolic fluxes to characterize the metabolic behaviors during initial and late growth phases. Highly active glycolysis fluxes and lower activity in TCA cycle fluxes were the characteristic feature for both phases. However, the metabolic flux distributions of pentose phosphate, amino acids and fatty acid biosynthetic pathways were high for initial exponential compared to the late exponential phase. Interestingly, when the glycerophospholipid pathway was explored, G3PC secreted during the late exponential (transitional) phase. This was highly consistent with our extracellular metabolite profiling results that showed the accumulation of G3PC during the transitional phase. Thus, the reduced activity of key metabolic pathways coupled with limited availability of intracellular G3PC could be associated with the reduction in cell growth rate in late exponential phase (see metabolic flux distribution details in Supplementary 4). The metabolic fluxes over amino acids biosynthetic pathways were also explored to understand the inter-conversion of asparagine into alanine and ammonia. First, asparagine was converted into glutamate via asparagine synthase (ASNS) and glutamate oxaloacetate transaminase 1 (GOT21). Subsequently, glutamate was transaminated to alanine via alanine aminotransferase (ALAAT) and ammonia via glutamate dehydrogenase (GDH), which was in good agreement with the experimental observation. In order to affirm confidence of the current
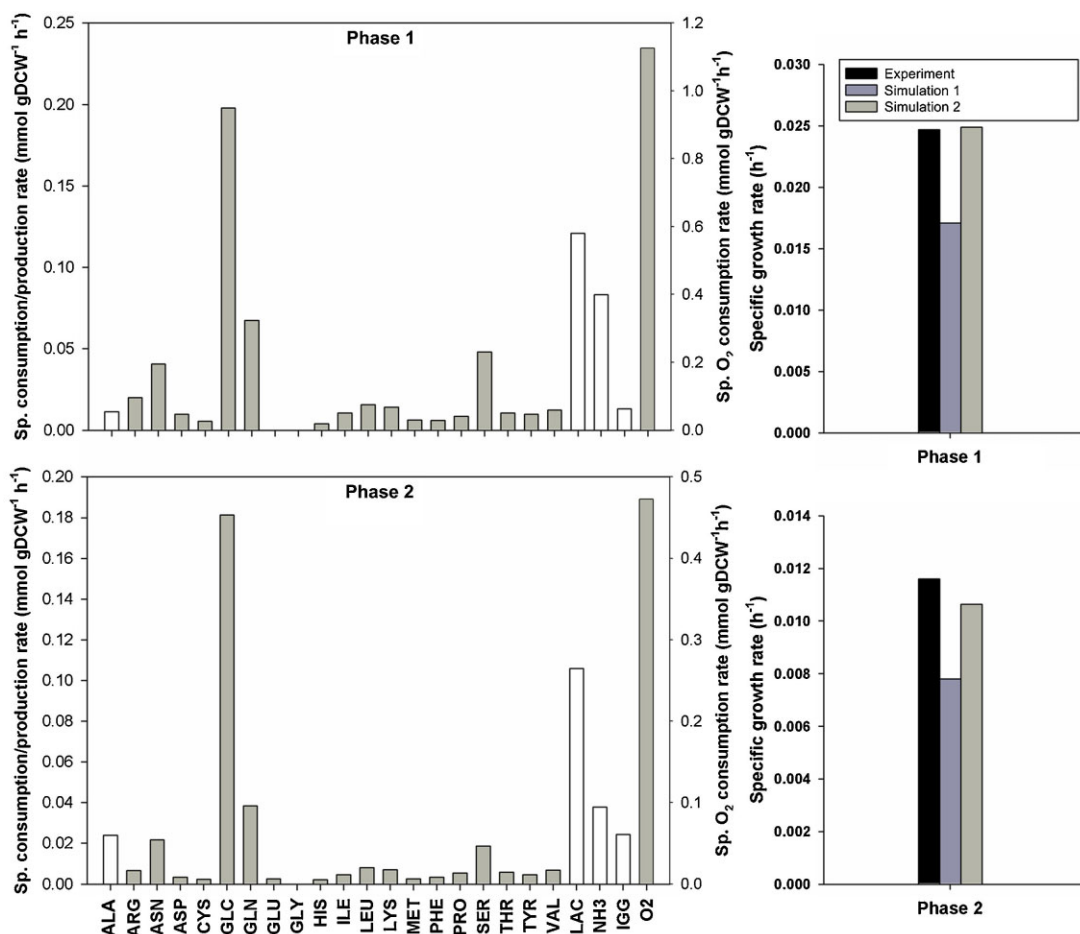
Figure 6. Comparison of in silico growth rate with experimentally observed growth rate during initial (phase 1) and late (phase 2) exponential phase of the culture. The bars with black and white colors represent specific consumption and production rates, respectively. Simulation 1 and 2 indicate predicted cell growth using amino acids content in biomass equation for mouse hybridoma and CHO M250-9 cells, respectively. [Color figure can be seen in the online version of this article, available at http://wileyonlinelibrary.com/bit]

simulation, we also conducted flux variability analysis (Mahadevan and Schilling, 2003) for initial exponential phase (P1). The results revealed 345 active reactions and their ranges of possible flux variations achieving the same phenotypic state (maximum cell growth) possibly through alternative pathways (see details in Supplementary 4). However, the small and consistent flux variation in central metabolism and very little or no variation in lipid and some amino acids pathways clearly indicated that the characteristic metabolic behavior discussed herein based on the simulated flux distributions would be highly plausible. Nevertheless, the actual flux determination must await experimental verification by isotope-based labeling measurements.

Non-Growth Phase

It is not appropriate to describe the stationary cellular phase by maximizing cell growth, as viable cell numbers tended to remain static, with either zero or negligible growth rates. Thus, we should consider an alternative approach to characterize the metabolic behavior during the non-growth phase. Based on previous studies, least square minimization (LSM) of error between experimental measurements and in silico simulations was successfully used to examine metabolic characteristics when the correct cellular objective could not be ascertained (Blank et al., 2005; Bonarius et al., 1996). Therefore, LSM was similarly applied in this study to evaluate the intracellular metabolic fluxes of CHO cells during the stationary culture phase. The uptake rates of measured nutrients and production rates of other by-products were first calculated as described earlier. Subsequently, LSM was conducted and the results indicated that flux distributions in energy and carbohydrate metabolism were similar to the growth phase. Although the cell growth was negligible during stationary phase, the consistent use of carbohydrate (glycolysis) pathways could be possibly utilized to meet energy demands arising from other cellular functions such as heat shock resistance and signal transduction. It is evident from the in silico simulations that further experiments aimed at examining the energy maintenance during the later phase of mammalian cell culture is worthwhile as it can provide clues to reengineer cells to enhance their viability, thereby optimizing recombinant productivity. Moreover, the results revealed significant reduction in metabolic fluxes of lipid and nucleotides pathways compared to their fluxes during exponential growth phase, suggesting that a slowdown in the activities of these pathways occurred during the non-growth culture phase. Additionally, in silico simulation also revealed the secretion of amino acid derivatives, which was consistent with the observed accumulation of these derivatives extracellularly based on the metabolomics analysis.

Discussion

This study describes how a combined metabolomics and modeling approach can be utilized to understand the intracellular behaviors of CHO cell culture. To date, the majority of mammalian cell culture studies focused on the analysis of extracellular glucose, lactate, glutamine, ammonia, and other amino acids. While these trends allow for an overview of cell metabolism, a more in-depth study of metabolites is required for better understanding of key intracellular mechanisms in relation to cell growth and death processes. As such, the extracellular and intracellular metabolite profiling studies have facilitated the detection of previously unmeasured metabolites, hence allowing for improved characterization of intracellular metabolic states. Specifically, the extracellular study resulted in the identification of previously unmeasured media components that were accumulating in the extracellular media. Additionally, a group of amino acid derivatives, nucleotides and other key metabolites were also found to build up extracellularly. This information could contribute towards improving the predictive capability of the CHO cell metabolic model, particularly during the non-growth culture phase.

The intracellular metabolite profiling study allowed us to identify key pathways potentially associated with cell growth limitation; metabolites participating in the energy, glutathione and glycerophospholipid metabolic pathways were found to show decreasing trends as the culture progressed. To derive a better understanding of this behavior, the corresponding fluxes for the three pathways were investigated using the in silico CHO model (Fig. 7). In terms of energy metabolism, the fluxes in the TCA cycle appear to be distinctly smaller than those of glycolysis. This is in good agreement with the largely known fact that glycolysis is the main energy production pathway in CHO cells, with build-up of lactate extracellularly (Xie and Wang, 1996). Additionally, the TCA cycle fluxes reduced from the late-exponential phase, further decreasing its contribution towards cellular energy production during the later culture phases.

Glutathione metabolism has been previously reported to be associated with the removal of reactive oxygen species in mammalian cells (O'Donovan and Fernandes, 2000). The intracellular metabolite profiling study revealed decreasing trends for both GSH and GSSG, while the latter was also shown to accumulate extracellularly, thereby suggesting that GSSG was secreted from the cells as the culture progressed. This observation was supported by in silico analysis results, shown by the positive transport flux of GSSG to the extracellular media in Figure 7. Interestingly, the results also indicated that the GSH formation flux, based on the conversion of glycine, glutamate, and cysteine via the enzymes D-aminoacid oxidase and aldehyde dehydrogenase, was relatively less during the later culture phases in comparison to the early exponential phase. This suggested that in order to maintain the reductive-oxidative potential intracellularly, GSSG had to be expelled from the cells. In addition, the reduction in the intracellular GSH pool also coincided with the transition of the cultures from exponential phase to stationary phase, which implied that the cells could have been undergoing oxidative stress due to
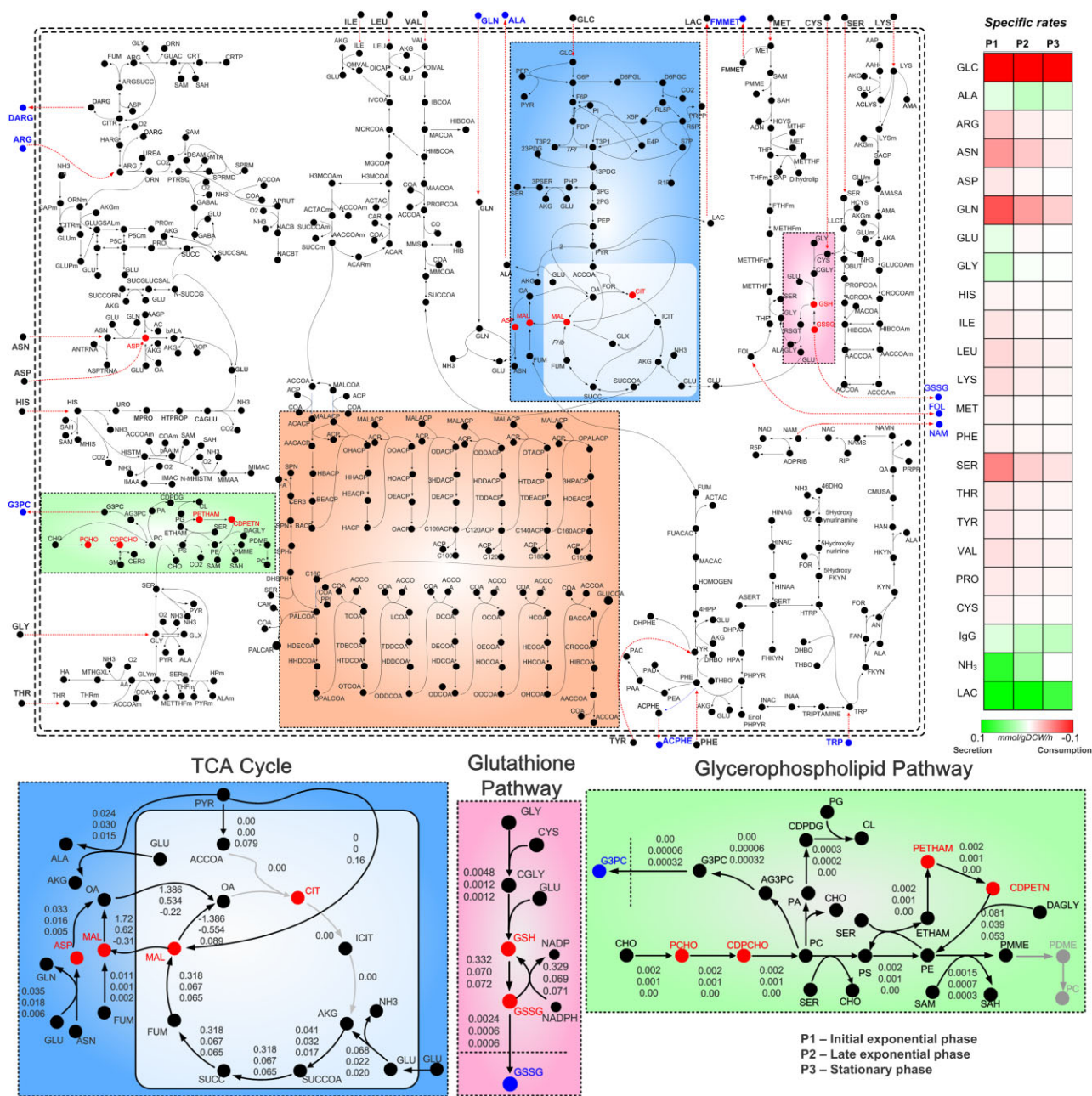
Figure 7. Schematic representation of the major metabolic pathways in CHO cell network. Pathways highlighted in different colors correspond to Glycolysis and TCA cycle (blue), Glutathione (magenta), lipid (orange), and glycerophospholipid (green) metabolisms. Specific consumption/production rates of major nutrients/products during three different cell culture phases are provided for the TCA cycle, glutathione, and glycerophospholipid metabolisms below. The given flux values have been determined under growth (P1, P2) and non-growth (P3) conditions. Depleting intracellular and accumulating extracellular metabolites are highlighted in red and blue colors, respectively.

the reduced availability of GSH (Hayes and McLellan, 1999). These observations suggest that oxidative stress could be a potential cause of cellular apoptosis and growth limitation in the fed-batch cultures. Thus, strategies to attenuate oxidative stress by adding antioxidants, e.g., butylated hydroxyanisole, *N*-acetylcysteine or ascorbic acid (Malhotra et al., 2008), could be evaluated for the enhanced cell growth and culture performance, in conjunction with metabolic

engineering of specific enzymes to better control the intracellular redox environment (Jo et al., 2001; Krishnan et al., 2008).

Glycerophospholipid metabolism was also found to be associated with growth limitation, based on the results of the intracellular metabolite profiling study, which revealed downward trends for several pathway intermediates (Table II). Both PC and PE are key constituents of the

plasma membrane and intracellular transport vesicles; hence, their synthesis is likely to be an important factor for cell growth and protein production. In particular, CDPCHO and CDPETN, the direct precursors to PC and PE, respectively, were found to be depleted during the exponential-stationary phase transition period. It should be highlighted that in silico analysis of CHO model allowed us to characterize metabolic states in the glycerophospholipid pathway. An overall reduction in the glycerophospholipid pathway fluxes was observed during the late exponential and stationary phases in comparison to the initial exponential phase (Fig. 7). In particular, the fluxes for the conversion of PCHO to CDPCHO and PETHAM to CDPETN were both zero in the stationary phase, suggesting that the synthesis of the PC and PE precursors could indeed have become limiting. A closer look at the fluxes also indicated that G3PC was being secreted continuously after the initial exponential phase of the culture, resulting in its accumulation extracellularly. These combined trends appear to point towards a slowdown in the production of PC and PE, which may potentially initiate the transition of cells to the stationary phase. However, more in-depth studies are required to further evaluate this hypothesis and to identify possible causes of the flux reductions in PC and PE synthesis. For instance, a potential focus could be on investigating the presence of enzymatic bottlenecks at the PCHO to CDPCHO and the PETN to CDPETN junctions in the pathway. This would enable the development of strategies to maintain PC and PE synthesis, which could subsequently lead to the extension of culture viability and in turn, improved culture performance.

From the discussion of the abovementioned metabolic pathways, the simulated fluxes derived from the in silico model have been successfully utilized to improve our understanding of key metabolic pathways presumably associated with the cell growth limitation. However, the current model has not accounted for compartment localization other than cytosol and mitochondria. Thus, inclusion of compartmental information could be beneficial, particularly, for investigating protein glycosylation mechanism with metabolic details corresponding to golgi and endoplasmic reticulum. Further improvements to the model can be made based on the recent availability of the CHO-K1 genome (Xu et al., 2011), in which the authors focused specifically on important gene functions relevant to protein glycosylation. With this information, glycosylation genes can be investigated using the metabolic model, which would eventually lead to enhancing the protein quality of recombinant therapeutics. Besides this, the consortium for CHO Cell Genomics, established by the Bioprocessing Technology Institute of Singapore and University of Minnesota in 2006 (Jayapal et al., 2007), has built a repertoire of approximately 80,000 EST sequences obtained from both traditional Sanger sequencing and next generation sequencing technologies such as Roche 454 and Solexa Illumina (Kantardjieff et al., 2009). This collection of ESTs can be subsequently used to examine the transcriptional activity of CHO cells. In the future, CHO specific genome sequences could be annotated with the availability of large amount of data. Such identified gene function from annotations can be added to improve the metabolic model representing CHO metabolism more precisely. Thus, the current limitations of the model can be overcome and it can be employed to identify strategies for cellular engineering.

Concluding Remarks

Mammalian cells are widely used for industrial production of recombinant therapeutics owing to their ability to perform post-translational modifications, including glycosylation. In this work, a combined metabolomics and in silico modeling approach was used to improve understanding of the intracellular mechanisms of CHO fed-batch cultures. Metabolites associated with cell growth limitation were first shortlisted based on both extracellular and intracellular metabolite profiling studies. A metabolic model representing the key metabolic functions of CHO cells was also developed using a template mouse genome-scale model and subsequently improved through integration of the extracellular metabolite profiling data. The in silico analysis of different fed-batch culture phases additionally highlighted the importance of obtaining accurate amino acid compositions in cell biomass. Finally, three key metabolic functions, including energy, glutathione, and glycerophospholipid pathways, potentially associated with cell growth limitation were studied in detail. Additional insights into these pathways were gained successfully based on the combined analysis of the experimental metabolite trends and the flux data obtained from the in silico model. In future, such an understanding could potentially facilitate the development of additional metabolic strategies for improvement of CHO cell culture productivity.

References

Altamirano C, Illanes A, Casablancas A, Gamez X, Cairo JJ, Godia C. 2001. Analysis of CHO cells metabolic redistribution in a glutamate-based defined medium in continuous culture. Biotechnol Prog 17:1032–1041.

Barnes LM, Dickson AJ. 2006. Mammalian cell factories for efficient and stable protein expression. Curr Opin Biotechnol 17(4):381–386.

Blank L, Kuepfer L, Sauer U. 2005. Large-scale 13C-flux analysis reveals mechanistic principles of metabolic network robustness to null mutations in yeast. Genome Biol 6(6).

Boger RH, Bode-Boger SM, Tsao PS, Lin PS, Chan JR, Cooke JP. 2000. An endogenous inhibitor of nitric oxide synthase regulates endothelial adhesiveness for monocytes. J Am Coll Cardiol 36(7):2287–2295.

Bonarius HPJ, Hatzimanikatis V, Meesters KPH, de Gooijer CD, Schmid G, Tramper J. 1996. Metabolic flux analysis of hybridoma cells in different culture media using mass balances. Biotechnol Bioeng 50(3):299–318.

Butler M. 2005. Animal cell cultures: Recent achievements and perspectives in the production of biopharmaceuticals. Appl Microbiol Biotechnol 68(3):283–291.

Carnicer M, Baumann K, Toplitz I, Sanchez-Ferrando F, Mattanovich D, Ferrer P, Albiol J. 2009. Macromolecular and elemental composition analysis and extracellular metabolite balances of *Pichia pastoris* growing at different oxygen levels. Microb Cell Factories 8:65.

Carvalhal AV, Santos SS, Calado J, Haury M, Carrondo MJ. 2003. Cell growth arrest by nucleotides, nucleosides and bases as a tool for improved production of recombinant proteins. Biotechnol Prog 19(1):69–83.

Chen XG, Wang RS, Deng MX, Ran XZ. 2005. Effects of exogenerous nucleotides on the apoptosis of intestinal epithelial cells IEC-6. Wei Sheng Yan Jiu 34(6):701–704.

Chong WP, Goh LT, Reddy SG, Yusufi FN, Lee DY, Wong NS, Heng CK, Yap MG, Ho YS. 2009. Metabolomics profiling of extracellular metabolites in recombinant Chinese hamster ovary fed-batch culture. Rapid Commun Mass Spectrom 23(23):3763–3771.

Chong WPK, Reddy SG, Yusufi FNK, Lee D-Y, Wong NSC, Heng CK, Yap MGS, Ho YS. 2010. Metabolomics-driven approach for the improvement of Chinese hamster ovary cell growth: Overexpression of malate dehydrogenase II. J Biotechnol 147(2):116–121.

Chong WP, Yusufi FN, Lee DY, Reddy SG, Wong NS, Heng CK, Yap MG, Ho YS. 2011. Metabolomics-based identification of apoptosis-inducing metabolites in recombinant fed-batch CHO culture media. J Biotechnol 151(2):218–224.

Chusainow J, Yang YS, Yeo JH, Toh PC, Asvadi P, Wong NS, Yap MG. 2009. A study of monoclonal antibody-producing CHO cell lines: What makes a stable high producer? Biotechnol Bioeng 102(4):1182–1196.

Covert MW, Famili I, Palsson BO. 2003. Identifying constraints that govern cell behavior: A key to converting conceptual to computational models in biology? Biotechnol Bioeng 84(7):763–772.

Dinnis DM, James DC. 2005. Engineering mammalian cell factories for improved recombinant monoclonal antibody production; lessons from nature? Biotechnol Bioeng 91(2):180–189.

Duarte NC, Becker SA, Jamshidi N, Thiele I, Mo ML, Vo TD, Srivas R, Palsson BO. 2007. Global reconstruction of the human metabolic network based on genomic and bibliomic data. Proc Natl Acad Sci 104(6):1777–1782.

Edwards JS, Palsson BO. 1998. How will bioinformatics influence metabolic engineering? Biotechnol Bioeng 58(2–3):162–169.

Filomeni G, Rotilio G, Ciriolo MR. 2003. Glutathione disulfide induces apoptosis in U937 cells by a redox-mediated p38 MAP kinase pathway. FASEB J 17(1):64–66.

Genzel Y, Friffer JB, Konig S, Alt R, Reichl U. 2005. Substitution of glutamine by pyruvate to reduce ammonia formation and growth inhibition of mammalian cells. Biotechnol Prog 21:58–69.

Hansen HA, Emborg C. 1994. Extra- and intracellular amino acid concentrations in continuous Chinese hamster ovary cell culture. Appl Microbiol Biotechnol 41(5):560–564.

Hayes JD, McLellan LI. 1999. Glutathione and glutathione-dependent enzymes represent a co-ordinately regulated defence against oxidative stress. Free Radic Res 31(4):273–300.

Jayapal KP, Wlaschin KF, Yap MGS, Hu W-S. 2007. Recombinant protein therapeutics from CHO cells-20 years and counting. Chem Eng Prog 103(7):40–47.

Jiang DJ, Jia SJ, Dai Z, Li YJ. 2006. Asymmetric dimethylarginine induces apoptosis via p38 MAPK/caspase-3-dependent signaling pathway in endothelial cells. J Mol Cell Cardiol 40(4):529–539.

Jo SH, Son MK, Koh HJ, Lee SM, Song IH, Kim YO, Lee YS, Jeong KS, Kim WB, Park JW, Song BJ, Huh TL. 2001. Control of mitochondrial redox balance and cellular defense against oxidative damage by mitochondrial NADP+-dependent isocitrate dehydrogenase. J Biol Chem 276(19):16168–16176.

Kantardjieff A, Nissom PM, Chuah SH, Yusufi F, Jacob NM, Mulukutla BC, Yap M, Hu W-S. 2009. Developing genomic platforms for Chinese hamster ovary cells. Biotechnol Adv 27(6):1028–1035.

Krishnan N, Dickman MB, Becker DF. 2008. Proline modulates the intracellular redox environment and protects mammalian cells against oxidative stress. Free Radic Biol Med 44(4):671–681.

Lee YY, Yap MGS, Hu W-S, Wong KTK. 2003. Low-glutamine fed-batch cultures of 293-HEK serum-free suspension cells for adenovirus production. Biotechnol Prog 19(2):501–509.

Lee SY, Lee D-Y, Kim TY. 2005. Systems biotechnology for strain improvement. Trends Biotechnol 23:349–358.

Lee JM, Gianchandani EP, Papin JA. 2006. Flux balance analysis in the era of metabolomics. Brief Bioinform 7(2):140–150.

Ma H, Zeng A-P. 2003. Reconstruction of metabolic networks from genome data and analysis of their global structure for various organisms. Bioinformatics 19(2):270–277.

Ma N, Ellet J, Okediadi C, Hermes P, McCormick E, Casnocha S. 2009. A single nutrient feed supports both chemically defined NS0 and CHO fed-batch processes: Improved productivity and lactate metabolism. Biotechnol Prog 25(5):1353–1363.

Mahadevan R, Schilling CH. 2003. The effects of alternate optimal solutions in constraint-based genome-scale metabolic models. Metabolic Eng 5(4):264–276.

Malhotra JD, Miao H, Zhang K, Wolfson A, Pennathur S, Pipe SW, Kaufman RJ. 2008. Antioxidants reduce endoplasmic reticulum stress and improve protein secretion. Proc Natl Acad Sci 105(47):18525–18530.

Miller W, Wilke C, Blanch H. 1988. Transient responses of hybridoma metabolism to changes in the oxygen supply rate in continuous culture. Bioprocess Biosyst Eng 3(3):103–111.

Mo M, Palsson BO, Herrgard M. 2009. Connecting extracellular metabolomic measurements to intracellular flux states in yeast. BMC Syst Biol 3(1):37.

O'Callaghan PM, James DC. 2008. Systems biotechnology of mammalian cell factories. Brief Funct Genomic Proteomic 7(2):95–110.

O'Donovan DJ, Fernandes CJ. 2000. Mitochondrial glutathione and oxidative stress: Implications for pulmonary oxygen toxicity in premature infants. Mol Genet Metabol 71(1–2):352–358.

Price ND, Papin JA, Schilling CH, Palsson BO. 2003. Genome-scale microbial in silico models: The constraints-based approach. Trends Biotechnol 21:162–169.

Price ND, Reed JL, Palsson BO. 2004. Genome-scale models of microbial cells: Evaluating the consequences of constraints. Nat Rev Microbiol 2:886–897.

Raghunathan AU, Pérez-Correa JR, Bieger LT. 2003. Data reconciliation and parameter estimation in flux-balance analysis. Biotechnol Bioeng 84(6):700–709.

Reff ME. 1993. High-level production of recombinant immunoglobulins in mammalian cells. Curr Opin Biotechnol 4(5):573–576.

Rossignol P, Collier S, Bush M, Shaw P, Doonan JH. 2007. Arabidopsis POT1A interacts with TERT-V(I8), an N-terminal splicing variant of telomerase. J Cell Sci 120(Pt 20):3678–3687.

Schaub J, Clemens C, Schorn P, Hildebrandt T, Rust W, Mennerich D, Kaufmann H, Schulz TW. 2009. CHO gene expression profiling in biopharmaceutical process analysis and design. Biotechnol Bioeng 105(2):431–438.

Selvarasu S, Wong VVT, Karimi IA, Lee D-Y. 2009. Elucidation of metabolism in hybridoma cells grown in fed-batch culture by genome-scale modeling. Biotechnol Bioeng 102(5):1494–1594.

Selvarasu S, Karimi IA, Ghim GH, Lee DY. 2010a. Genome-scale modeling and in silico analysis of mouse cell metabolic network. Mol Biosyst 6(1):142–151.

Selvarasu S, Kim DY, Karimi IA, Lee DY. 2010b. Combined data preprocessing and multivariate statistical analysis characterizes fed-batch culture of mouse hybridoma cells for rational medium design. J Biotechnol 150(1):94–100.

Smith CA, Want EJ, O'Maille G, Abagyan R, Siuzdak G. 2006. XCMS: Processing mass spectrometry data for metabolite profiling using nonlinear peak alignment, matching, and identification. Anal Chem 78(3):779–787.

Tsao YS, Cardoso AG, Condon RGG, Voloch M, Lio P, Lagos JC, Kearns BG, Liu Z. 2005. Monitoring Chinese hamster ovary cell culture by the analysis of glucose and lactate metabolism. J Biotechnol 118(3):316–327.

Wahl A, Sidorenko Y, Dauner M, Genzel Y, Reichl U. 2008. Metabolic flux model for an anchorage-dependent MDCK cell line: Characteristic growth phases and minimum substrate consumption flux distribution. Biotechnol Bioeng 101(1):135–152.

Xie L, Wang DIC. 1994. Stoichiometric analysis of animal cell growth and its application in medium design. Biotechnol Bioeng 43(11):1164–1174.

Xie L, Wang DIC. 1996. Energy metabolism and ATP balance in animal cell cultivation using a stoichiometrically based reaction network. Biotechnol Bioeng 52(5):591–601.

Xu X, Nagarajan H, Lewis NE, Pan S, Cai Z, Liu X, Chen W, Xie M, Wang W, Hammond S, Andersen MR, Neff N, Passarelli B, Koh W, Fan HC,

Wang J, Gui Y, Lee KH, Betenbaugh MJ, Quake SR, Famili I, Palsson BO, Wang J. 2011. The genomic sequence of the Chinese hamster ovary (CHO)-K1 cell line. Nat Biotechnol 29(8):735–741.

Yizhak K, Benyamini T, Liebermeister W, Ruppin E, Shlomi T. 2010. Integrating quantitative proteomics and metabolomics with a genome-scale metabolic network model. Bioinformatics 26(12):i255–i260.

Zablocki K, Miller SP, Garcia-Perez A, Burg MB. 1991. Accumulation of glycerophosphocholine (GPC) by renal cells: Osmotic regulation of GPC:choline phosphodiesterase. Proc Natl Acad Sci 88(17):7820–7824.

Zupke C, Stephanopoulos G. 1995. Intracellular flux analysis in hybridomas using mass balances and in vitro ^{13}C NMR. Biotechnol Bioeng 45(4):292–303.